Hospital Evacuation Planning Tool for Assistance Devices (HEPTAD)

Michael Joyce, Peter J Lawrence & Edwin R Galea, Fire Safety Engineering Group, University of Greenwich, UK

ABSTRACT

A new software tool, called HEPTAD (Hospital Evacuation Planning Tool for Assistance Devices), designed to aid evacuation planning in hospitals is described and demonstrated in this paper. The software can identify regions within a hospital geometry that are inappropriate for patients who require the use of specific movement assistance devices in the event of an emergency evacuation. Using the software, Hospital Emergency Coordinators can reduce the risk of allocating a bed to a patient from which they cannot be evacuated within a safe time. In addition, HEPTAD is designed to be a proof of concept for algorithms that will later be incorporated within the EXODUS egress model. HEPTAD utilises several techniques from autonomous robotics to generate the fastest viable egress route for movement assistance devices from every location in the geometry while considering device spatial constraints (size and shape) and kinematic constraints (maximum speeds, turning radius and holonomicity). It then uses the egress time of this route along with factors from space syntax (isovist and spaciousness) to analyse the emergency vulnerability of every location within the geometry.

INTRODUCTION

Between April 2010 and April 2018, there was an average of approximately 750 serious fires in hospitals and medical care facilities per year in England alone and on average one fire-related casualty in every 20 of these fires [1]. Many fires in hospitals require a progressive horizontal evacuation of patients to a neighbouring fire compartment with the use of their hospital bed. However, full evacuations of hospitals are sometimes required, such as the 2008 Royal Marsden fire in London, UK [2,3] and the 16 full evacuations of hospitals after the 2016 Kumamoto earthquake in Japan [4]. Many of these evacuations required the vertical movement of patients with specialised movement assistance devices due to their mobility requirements. Therefore, the success of full evacuations depends greatly on assistance from staff and their use of these devices [5].

It is widely agreed that evacuation plans and the layout of hospital facilities should be designed with movement assistance devices in mind [6,7]. It is therefore critical to fully understand the variety of assistance devices in use to develop effective evacuation plans. These assistance devices, such as evacuation chairs, hospital beds, wheelchairs, rescue sheets and stretchers, vary significantly in terms of their spatial constraints (size and shape) and kinematic constraints (movement speed, acceleration and manoeuvrability) [3,8,9]. This means the route with the shortest evacuation time from each room may differ depending on the device in use. Therefore, current factors used to determine shortest evacuation routes throughout a geometry, such as the position of fire hazards and the presence of other evacuating occupants, may not be sufficient and device constraints should also be taken into account. In addition, the impact of fire hazards

on viable exit routes may be dependent on the nature of the device employed due to various performance constraints associated with the device.

Patients who require the use of specific assistance devices during an evacuation must not be located in areas where they cannot be manoeuvred to an exit / safe area in less time than the ASET (Available Safe Egress Time [10]) of the scenario when using the device. These inappropriate areas can be estimated by analysing the egress time required with the use of the device in the absence of interactions with other evacuating occupants.

The research presented here outlines a new technique for obtaining an *Individual Value of Emergency Vulnerability* (IVEV) for every point in a building geometry. This has been implemented into a software tool named HEPTAD (Hospital Evacuation Planning Tool for Assistance Devices) that can aid Hospital Emergency Coordinators (HECs) by determining the areas of the geometry that are inappropriate for patients based on the assistance devices used. The IVEV is calculated for each type of assistance device by assessing the viable egress routes for the device from every point in the geometry.

The tool can also be utilised to test the suitability of egress routes for an assistance device under different scenarios as part of a risk assessment exercise (such as a Qualitative Design Review [7]) and determine alternative egress routes if the primary one becomes blocked. Furthermore, real-time applications of the methodology could be developed to identify alternative, viable, near-optimal evacuation routes during an actual incident should the preferred evacuation route be compromised. This has become particularly relevant in recent years due to a growing interest in developing autonomous robotic movement assistance devices, such as hospital beds [11,12], wheelchairs [12] and stretchers [13], that can be utilised to autonomously transport patients throughout hospitals during an evacuation. In addition to these applications, HEPTAD provides a proof of concept for theoretical models that will later be incorporated into the EXODUS egress model [14].

BACKGROUND

Many patients may have specific medical constraints which limit the type of assistance device that can be employed to take them to a place of safety during an emergency. As a result, Florida Department of Health [15] has suggested conducting a "patient movement study, based on the number and type of patient to be moved from which locations" to determine the distribution of devices throughout a hospital. There is, however, no guarantee that because a patient is near an appropriate assistance device, their egress time will be below the ASET. Therefore, it may be imperative to have one step before the patient movement study to first allocate beds to patients based on the expected egress time for an appropriate assistance device from that location.

To achieve an appropriate allocation of beds, it is essential to have a good understanding of the egress time for each device from every location within the geometry under likely evacuation scenarios. However, traditional methods to determine the egress time of assistance devices, such as drills or physical trials, can be costly, time-consuming and potentially hazardous [7]. Furthermore, given that hospitals and care homes are occupied 24 hours a day, any physical trial is often constrained by the requirements of the occupants. One solution is to use a modelling approach; however, HECs have relied on limited modelling tools to plan for the use

and distribution of devices [6,16]. These tools have consisted of several hand calculation and simulation models that have limitations in their scope and accuracy.

Two hand calculation models have been developed to assess the vulnerability of areas of a geometry during an evacuation. The first, developed by Ünlü et al [17], has used several space syntax variables to give an estimate of the vulnerability of each area in the geometry. However, this model does not consider routes that are viable for People with Reduced Mobility (PRM) and instead assumes a homogenous population. Taking this one step further, the second model, by Hashemi [18], has calculated an *accessibility index* for each corridor, ramp, doorway, stairway and lift in the geometry for wheelchair users based on a weighted sum of relevant variables for each entity (such as the width and length of a corridor and the width of a doorway). A coarse network has then been constructed with each arc representing a corridor, ramp, doorway, stairway or lift and each node representing junctions between two arcs. Dijkstra's algorithm [19] has then been used to find the egress route that minimises the total accessibility index from each node in the geometry. These models, however, do not differentiate between assistance devices that may be utilised during an evacuation so cannot be used to determine which devices are suitable from different start locations.

To determine the most suitable assistance devices for a hospital, there have been only two hand calculation tools made available to HECs. The first, by the United States Department of Homeland Security [20], has provided a metric for analysing the performance of possible assistance devices based on a weighted sum of several subjective factors obtained from focus groups. The second, by Hunt et al [8,9], has provided a metric that also includes empirically obtained performance factors such as horizontal and vertical movement speeds, number of operators and space occupied. Neither of these tools, however, identify the unsafe areas of the hospital for each evacuating patient based on their mobility requirements.

Hunt [9] has also developed a theoretical model to analyse geometries and produce viable routes for assistance devices by taking into account their spatial constraints (size and shape). The model analyses the width of each corridor and narrow gap in the geometry and marks it as impassable if its width is less than the width of the device. The model goes on to mark any 90-degree corner as impassable by analytically determining if the device can traverse it based on its length and width. Thus, when attempting to find viable routes, Hunt's model represents assistance devices as rectangles for 90-degree corners and circles elsewhere. These spatial representations fail to consider any other shape that may restrict the available viable routes of a device. In addition, Hunt's model does not provide much additional information about the accessibility of routes for a compliant hospital geometry. This is because the minimum possible width of an egress route within a compliant hospital geometry in the UK is 1200mm for both hospital beds and general traffic (calculated from the Health Technical Memorandum 05-02 [7] and the Health Building Note 00-04 [21]) which is wider than a typical assistance device that may be utilised. In addition, any 90-degree corner in an egress route must be able to accommodate a hospital bed's length and width when a bed is used and a wheelchair's length and width (with an attendant) for general traffic. As assistance devices can generally be grouped into prone devices (such as stretchers and rescue sheets) with similar dimensions to a hospital bed or seated devices (such as, carry chairs and evacuation chairs) with similar dimensions to a wheelchair, any analysis of a compliant egress route with this model will likely return as passable for any of these assistance devices.

A potential problem with compliant egress routes that has been overlooked by Hunt's model [9] concerns the kinematic constraints of devices. These kinematic constraints dictate how an assistance device can manoeuvre through a geometry, further restricting available routes. The main kinematic constraints that impact an assistance device's manoeuvrability are its minimum turning radius and *holonomicity*. The holonomicity of a device is a measure of whether it can move in any direction without first rotating [22]. For example, a stretcher can move in any direction without the need to rotate, while a wheelchair will have to rotate to change direction (other than reversing). Thus, the stretcher, a holonomic device, is not as constrained as the wheelchair, a non-holonomic device. A non-holonomic device may not be able to traverse a 90-degree corner even if an analysis of its length and width by Health Building Note 00-04 [21] or Hunt's model [9] returns as passable. This limited representation of spatial and kinematic constraints in Hunt's model [9] may result in the prediction of unrealistic routes in some geometries leading to unreliable qualitative and quantitative results.

Hunt's model [9] has been implemented in the Pathfinder [23] and EXODUS [8,9,14] evacuation simulation models. Therefore, unlike most evacuation models that have been unable to represent assistance devices [3,9], Pathfinder and EXODUS have been able to explicitly represent *some* of the spatial constraints that have an impact on the route finding (and therefore egress time) of devices. Although they make use of the same methods for assistance devices, these models differ in the way they represent geometries. Pathfinder represents geometries as continuous spaces in which occupants, represented as circles, navigate using a navigation mesh [23]. By contrast, EXODUS discretises the geometry into a network of nodes and arcs arranged in a fine grid with a default spacing of 0.5 × 0.5 metres representing the space taken up by an occupant. Therefore, each node can be occupied by at most one occupant at a time and each occupant must occupy exactly one node. Each node is connected to its 8 (or less) neighbours with arcs allowing occupants to jump from node to node. Walls and obstacles are marked with boundary lines. Occupants move through this network towards an exit or goal using a potential map [14]. This network representation of the geometry is mirrored by HEPTAD. An example geometry as represented in EXODUS is shown in Figure 1.

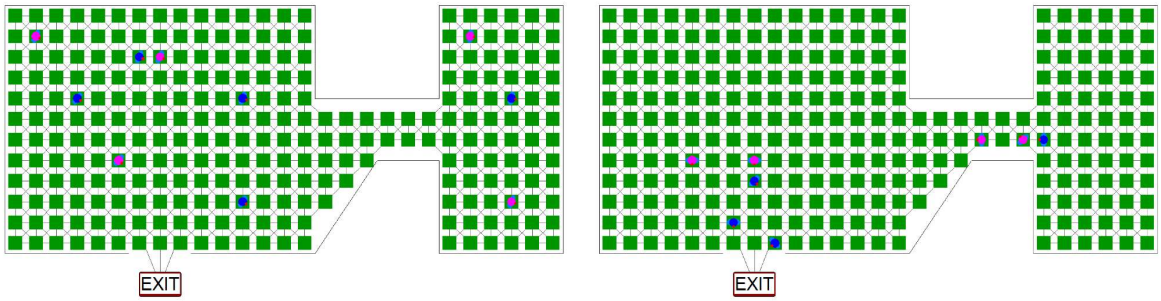

(a) Before simulation (a) During simulation

Figure 1: Example geometry in EXODUS with boundary lines (marking the walls of the geometry), nodes (green squares), arcs (connecting the nodes), occupants (blue and pink circles) and an exit.

In addition to the underlying limitations in Hunt's model [9], neither Pathfinder nor EXODUS has been able to predict the required egress time for an assistance device from every location in the geometry without individually simulating the movement from each location. This means,

although they have been used to verify an existing evacuation plan, they are inefficient at determining a safe distribution of patients within a hospital.

Ronchi et al [24] have suggested that features based on fields of study outside of fire safety engineering are often relevant to evacuation modelling. Following this principle, this research has looked at methods from two external fields of study, autonomous robotics and space syntax, with the aim to solve limitations with existing models and add functionality to the EXODUS egress model. Particular interest has been placed on recent work in the field of autonomous robotics, where, through the use of a network embedded in C-Space, the most relevant spatial and kinematic constraints of autonomous robots have been represented [25].

THEORETICAL MODEL

C-Space Network

The first method incorporated into HEPTAD is from the field of autonomous robotics and consists of representing each Degree Of Freedom (DOF) of the assistance device in a C-Space (configuration space) [22]. In this context (a 2D rigid body navigating a 2D geometry), the C-Space represents the collection of points describing every possible position and orientation of a given object within a given geometry. Every point in the C-Space, therefore, consists of an x and y co-ordinate describing the location of a reference point on the device and an angle representing the orientation of the device around this point. The C-Space is, therefore, a three-dimensional space. Multi-floor structures can be represented with this method by including an additional dimension isomorphic to $\mathbb{Z}$, representing the floor number. However, stairways are not yet represented in HEPTAD, so a three-dimensional space is utilised in this work. The method utilised in this research discretises this space into a network of nodes and arcs through which the device can navigate. This technique has been shown to work well when path planning for robots in "close proximity" environments, for example, an Improvised Explosive Device (IED) disposal robot [25]. This has an analogy to the movement of assistance devices through narrow corridors and doorways.

To construct the C-Space, the geometry is first represented as a collection of boundary lines marking out the walls and obstacles in the building. The version of HEPTAD presented in this paper is limited to single floor structures giving 3 DOF. These are the spatial coordinates of a reference point on the device (x and y position) and the angular orientation around this point (θ measured clockwise in degrees from the positive y axis). This means that any configuration (position and orientation) in the geometry can be represented by the three co-ordinates (x, y, θ). A 3D C-Space is constructed for each assistance device where every $(\tilde{x}, \tilde{y}, \tilde{z})$ coordinate in this space represents exactly one (x, y, θ) configuration in the geometry where $\tilde{x} = x$ [in metres], $\tilde{y} = y$ [in metres] and $\tilde{z} = \theta$ [in degrees]. Note that 0 is identified with 360 on the $\tilde{z}$ axis (i.e. it is modular 360) making it isomorphic to the unit circle S^1. An example of how configurations in the geometry are represented in C-Space is shown in Figure 2.

To enable the incorporation of spatial and kinematic constraints into C-Space, some form of discretisation must be performed on this space. To achieve this, a 3D network is embedded in the 3D C-Space. Each node n in this network has a position $(\tilde{x}, \tilde{y}, \tilde{z})$ in C-Space that corresponds to exactly one configuration (x, y, θ) in the geometry. The nodes are placed in a

3D grid with a spacing of 0.25×0.25 on the $\tilde{x}, \tilde{y}$ plane of and a spacing of 22.5 on the $\tilde{z}$ axis. The spacing on the $\tilde{x}, \tilde{y}$ plane is chosen to be twice the resolution of the default network structure in EXODUS so it can be obtained from this network by performing a *barycentric subdivision* [26]. This is to allow for easy communication between the nodes in HEPTAD and the nodes in EXODUS to prepare for merging the two models. The spacing on the $\tilde{z}$ axis provides 16 possible orientations. The number of orientations can be edited by changing this spacing.

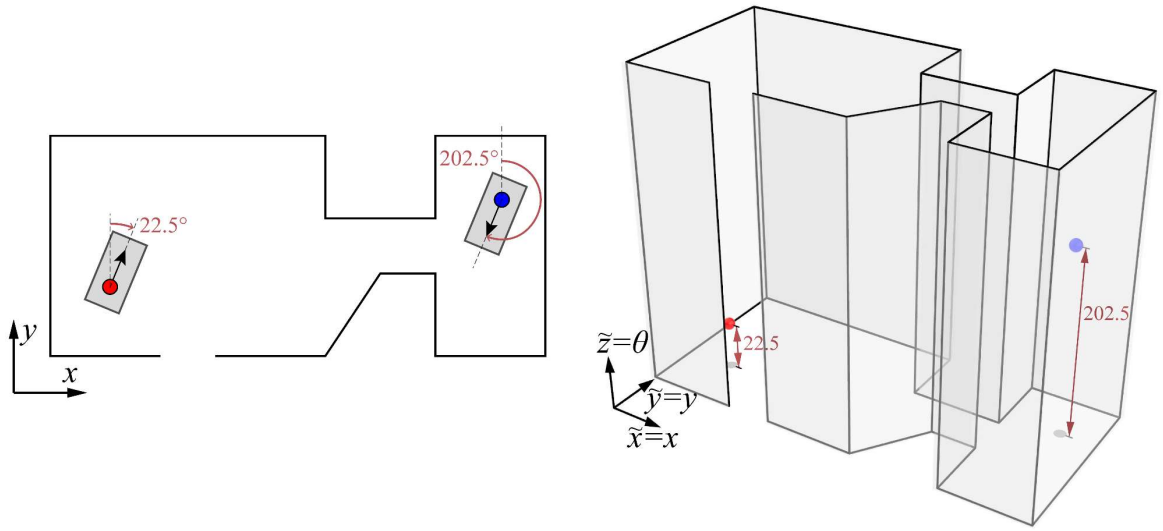

(a) Geometry (T-Space) (b) C-Space

Figure 2: Representation of the same two configurations of an assistance device (red and blue) as shapes in the geometry and points in C-Space.

For a geometry that can be contained in the rectangle $[E, W] \times [S, N] \subset \mathbb{R}^2$ on the real plane (for some $N, S, E, W \in \mathbb{R}$ with $E < W$ and $S < N$), a node is placed in C-Space at position $(0.25i, 0.25j, 22.5k)$ for all $i, j, k \in \mathbb{Z}$ such that $4E \leq i \leq 4W$, $4S \leq j \leq 4N$ and $0 \leq k < 16$. These nodes form a 3D grid with an $\tilde{x}$ spacing of 0.25, a $\tilde{y}$ spacing of 0.25 and a $\tilde{z}$ spacing of 22.5. The nodes can be viewed as a collection of 16 layers where each layer represents one θ orientation (i.e. one $\tilde{z}$ value). This structure is shown in Figure 3. Note that the network embedded in C-Space does not have to form a regular grid. Once HEPTAD is incorporated into EXODUS, the underlying 2D network in EXODUS can be utilised to construct a corresponding 3D network in HEPTAD.

To simplify notation, for two configurations $c_1 = (x_1, y_1, \theta_1)$ and $c_2 = (x_2, y_2, \theta_2)$, let $d_{x,y}(c_1, c_2) := \sqrt{(x_2 - x_1)^2 + (y_2 - y_1)^2}$ and $d_\theta(c_1, c_2) := \min(\theta_{2-1}, \theta_{1-2})$ where θ_{2-1} and θ_{1-2} are the smallest positive real numbers such that $\theta_1 + \theta_{2-1} \equiv \theta_2 \pmod{360}$ and $\theta_2 + \theta_{1-2} \equiv \theta_1 \pmod{360}$. In other words, $d_{x,y}(c_1, c_2)$ denotes the Euclidian distance between the x, y positions represented by c_1 and c_2 and $d_\theta(c_1, c_2)$ denotes the minimum amount of rotation between the θ orientations represented by c_1 and c_2 (anticlockwise or clockwise).

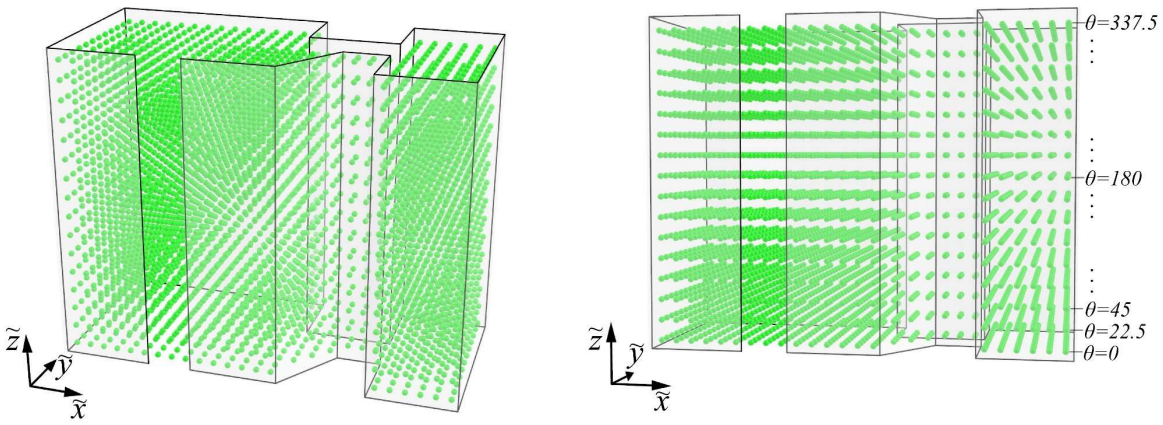

Figure 3: Two views of the 3D grid of nodes (represented as green spheres) embedded in C-Space for an example geometry. The nodes that lie outside of the geometry have been removed.

For all pairs of nodes n_1 and n_2 in the network that represent configurations c_1 and c_2 respectively, two directed arcs $a_1 = (n_1, n_2)$ and $a_2 = (n_2, n_1)$ are added between them if and only if $d_{x,y}(c_1, c_2) \leq \sqrt{0.25^2 + 0.25^2}$ and $d_\theta(c_1, c_2) \leq 22.5$. In other words, each node is connected to its 8 neighbours on the same layer (as shown in Figure 4 (a)), and the 9 nodes directly above and 9 nodes directly below these neighbours (as shown in Figure 4 (b)). This gives each non-boundary node a collection of arcs that corresponded to 8 linear directions and two angular directions (clockwise and anticlockwise) in the geometry. This results in 8 arcs that represent a linear movement with no rotation, 8 arcs that represent a linear movement with a clockwise rotation, 8 arcs that represent a linear movement with an anticlockwise rotation and 2 arcs that represent a rotation with no linear movement. This is a total of 26 directional arcs per non-boundary node.

Representing Constraints

The most relevant spatial constraints (size and shape) and kinematic constraints (turning radius and holonomicity) of an assistance device are represented by editing the C-Space network. Spatial constraints have been commonly represented in C-Space by taking the Minkowski sum [22] of the boundary lines with the device shape for each orientation. This can be thought of as shrinking the device down to a single point while inflating the boundary lines. The result of doing this is a 3D volume in C-Space that marks out the invalid configurations, i.e., the configurations that would result in a collision with a boundary line. As the representation of C-Space is discretised into a network, the nodes that sit inside this Minkowski sum (and therefore represent an invalid configuration) are removed from the network. All remaining nodes in the C-Space network represent valid configurations, that is, configurations that do not cause a collision with a boundary line.

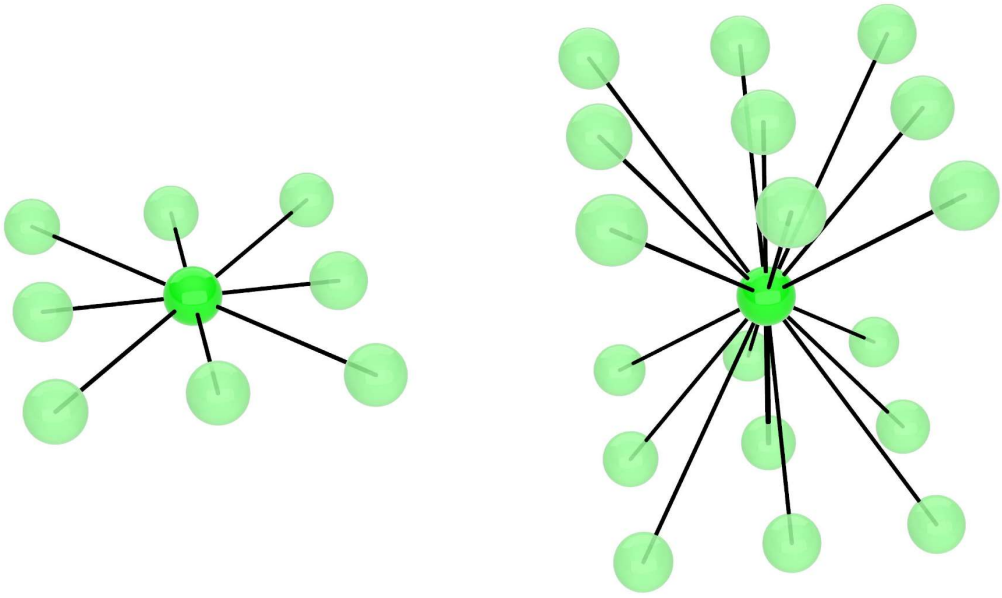

(a) Connections within same layer of C-Space

(b) Connections with layer above and below in C-Space

Figure 4: Connectivity of a node in C-Space.

The representation of the kinematic constraints is produced in a similar fashion by removing all directed arcs in the network that represented an invalid movement. If the device is unable to turn on the spot (has a non-zero minimum turning radius), all arcs that represent a rotation with no linear movement are removed. That is, all directed arcs that represent a movement from configuration (x_1, y_1, θ_1) to (x_2, y_2, θ_2) such that $x_1 = x_2$ and $y_1 = y_2$ are removed. To represent a non-holonomic device (in this context, a device whose linear movement direction must be equal to the direction it is facing), all arcs that cause a linear movement whose direction differs from the current orientation by more than some tolerance are removed. So, given a tolerance of ε degrees, an arc that represents a movement from configuration (x_1, y_1, θ_1) to (x_2, y_2, θ_2) is removed if the inequality in Equation 1 is true. A value of $\varepsilon = 22.5$ is used here to ensure that every movement direction is valid for at least one orientation. Figure 5 shows a sample of nodes in C-Space with the same $(\tilde{x}, \tilde{y})$ position with their connected arcs after this process has been performed. Note that there are 16 possible orientations but only 8 possible movement directions, hence some orientations will lie halfway between two movement directions. When this is the case, both movement directions will be valid. For example, when $\theta = 67.5°$ there are two possible movement directions from each node (45° and 90°) as they are both within the tolerance. This is shown in Figure 5.

$$d_\theta\left(\theta_1, tan^{-1}\left(\frac{d(x_1, x_2)}{d(y_1, y_2)}\right)\right) > \varepsilon \qquad [1]$$

Route Finding

One benefit of embedding a network in C-Space is that route-finding is relatively simple. Given the target nodes (exits) and appropriate weights for each arc, Dijkstra's shortest path algorithm [19] is used to determine the egress time from each node in the network and the quickest route from that node to an exit. Since the nodes and arcs that represent invalid configurations and

movements have been removed, the resulting routes automatically abide by the spatial and kinematic constraints of the device. This means after running Dijkstra's algorithm once on the C-Space network, a viable route is found from every start location in the geometry to the nearest exit, removing the need for repeated simulations from each start location.

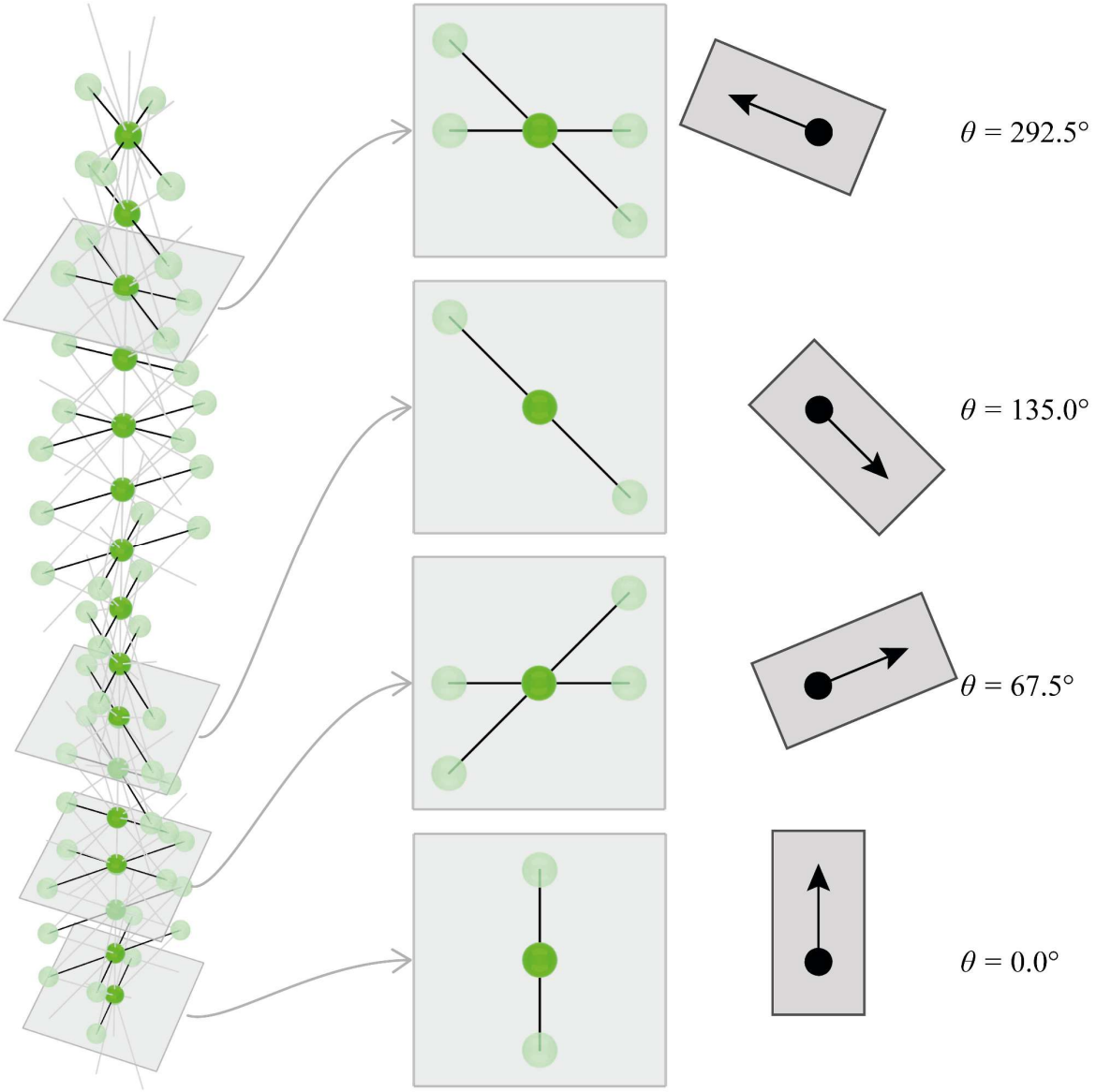

Figure 5: Remaining arcs for a non-holonomic device after kinematic constraints have been applied. Left: 16 nodes representing different orientations and the same $(\tilde{x}, \tilde{y})$ position with arcs connected to the same layer (black) and neighbouring layers (grey). Middle: 4 sections of the left figure. Right: corresponding orientation of the device for each section.

The weight of each arc takes into account the maximum linear speed ${s_L}^{max}$ and maximum angular speed ${s_A}^{max}$ of the assistance device. The weight of an arc a that represents a movement from configuration c_1 to c_2 is determined by Equation 2.

$$W(a) = \sqrt{\left(\frac{d_{x,y}(c_1, c_2)}{{s_L}^{max}}\right)^2 + \left(\frac{d_\theta(c_1, c_2)}{{s_A}^{max}}\right)^2} \quad [2]$$

The weight of each arc is the time taken for the device to move from the first configuration to the second under the assumption that this is equal to $\sqrt{t_L^2 + t_A^2}$ where t_L is the time taken to move the linear distance $d_{x,y}(c_1, c_2)$ at linear speed ${s_L}^{max}$ and t_A is the time taken to move the angular distance $d_\theta(c_1, c_2)$ at angular speed ${s_A}^{max}$. With these weightings, the resulting potential on each node from Dijkstra's algorithm is the time for the device to get from the configuration represented by that node to the nearest exit travelling at its maximum linear and angular speeds. Acceleration and deceleration are also considered by increasing the weight of an arc during Dijkstra's algorithm when the direction of the current shortest path changes. This takes the slowing of the device into account when it changes movement direction. This method is an extension of that used by Hashemi [18] to decrease the accessibility of an egress route in the geometry every time it traverses a corner. The potential on each node after Dijkstra's algorithm is the time taken for the device to get from the configuration represented by the node to the nearest exit.

Individual Value of Emergency Vulnerability (IVEV)

The concept of a Value of Emergency Vulnerability (VEV), proposed by Ünlü et al [17], has, in the past, taken into account 5 factors; *real integration* (a measure of how isolated the location is), *isovist* (area of geometry visible from the location), *distance* (distance to an exit), *queuing crowd* (density of people in the location) and *spaciousness* (how much space is available around the location i.e. the floor area of the room containing the location). For each location in the geometry, HEPTAD calculates the spaciousness and isovist factors and utilises the egress time from this location (or nearest node in C-Space) to represent both the real integration and distance factors. The queuing crowd factor will be represented by the interactions with occupants when the HEPTAD algorithms are incorporated into EXODUS. Therefore, as the interactions with other occupants are not currently taken into account, HEPTAD produces the Individual Value of Emergency Vulnerability (IVEV) for every position in the geometry and not the full VEV.

To gain a value for each of the three factors (egress time, spaciousness and isovist), the 2D floor plan is discretised into $0.25m \times 0.25m$ cells so that the centre of each cell has the same (x, y) position as the $(\tilde{x}, \tilde{y})$ position of nodes in C-Space, i.e., at $(0.25i, 0.25j)$ for all $i, j \in \mathbb{Z}$ such that $4E \leq i \leq 4W$ and $4S \leq j \leq 4N$. This means that each cell corresponds to at most 16 nodes in C-Space with the same $(\tilde{x}, \tilde{y})$ coordinates. This number will be less than 16 if some of the nodes were deleted when representing the spatial constraints. The cells for an example geometry are shown in Figure 6. The egress time T of a cell is the average egress time (in seconds) over these nodes. The isovist I is the total area (in metres squared) visible from the centre of the cell, calculated by casting rays from the centre of the cell and testing for intersections with boundary lines. Each ray has a maximum length equal to a maximum visibility distance v. The spaciousness S is a measure of the proportion of valid orientations at the position represented by the centre of the cell, calculated by taking the total number of nodes that correspond to the cell (that have not been deleted) and dividing by 16.

To calculate the IVEV, a dimensionless value is constructed for each factor then a weighted sum is taken. The dimensionless values lie between 0 and 1 such that 0 is the least vulnerable for that factor and 1 is the most vulnerable. The dimensionless egress time is $\hat{T} = \frac{T}{ASET - Prep. - Resp.}$ where *ASET* is the available safe egress time (obtained from fire models or risk assessments), *Prep.* is the preparation time for the assistance device and *Resp.* is the longest possible response time of staff. The dimensionless spaciousness is $\hat{S} = 1 - S$. Finally, the dimensionless isovist is $\hat{I} = 1 - \frac{I}{\pi v^2}$ where v is the maximum visibility distance. With these values, the IVEV is calculated with Equation 3 where weights w_T, w_S and w_I (such that $w_T + w_S + w_I = 1$) represent how much the egress time, spaciousness and isovist factors (respectively) influence the vulnerability of a location. Weights of $w_T = 0.7$, $w_S = 0.1$ and $w_I = 0.2$ are used here for demonstration purposes.

$$\text{IVEV} = w_T\hat{T} + w_S\hat{S} + w_I\hat{I} \quad [3]$$

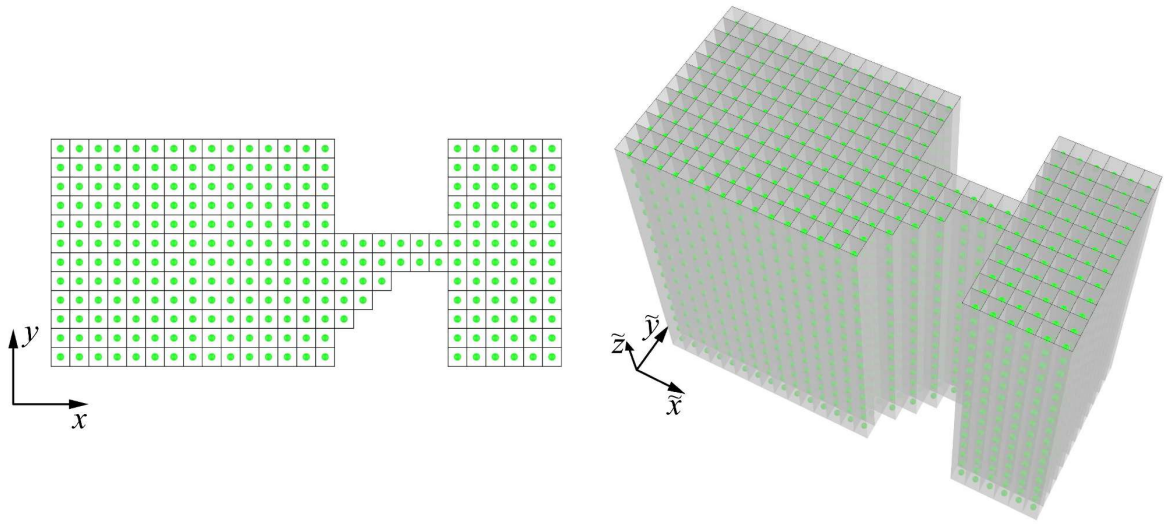

Figure 6: Discretisation of geometry into cells with centre equal to the (x, y) position of nodes. Cells are shown in the geometry (left) and C-Space (right).

Hazards

Hazards (such as fire, smoke or debris) are represented in HEPTAD as regions of the geometry where the assistance device cannot go. Once their position is defined in the geometry, they can be made active or inactive and the egress routes are recalculated accordingly giving new egress times and, therefore, IVEVs. Note that HEPTAD assesses the vulnerability of locations in the geometry during an evacuation and does *not* assess the likelihood of an evacuation taking place. Therefore, each hazard receives a probability value that is a prediction of the likelihood the hazard is active *given* an evacuation is taking place. This probability can be predicted through risk assessment exercises. The model assumes that at most one hazard can be active at any time, so the sum of the probabilities of the hazards must be ≤ 1. For n hazards $H_1, H_2, \ldots, H_n$ with respective probabilities $P_1, P_2, \ldots, P_n$, the empty hazard H_0 representing no hazard (for example in a non-emergency evacuation) has a probability $P_0 = 1 - \sum_{i=1}^{n} P_i$.

With this probability measure, a weighted average of the IVEV is calculated called the *averaged Individual Value of Emergency Vulnerability* (aIVEV). To simplify notation, let $T(i)$ and $\mathrm{IVEV}(i)$ denote the egress time and IVEV of a cell (respectively) with hazard i active. For each cell, the aIVEV over all hazards is calculated using Equation 4.

$$\mathrm{aIVEV} = \sum_{i=0}^{n} \mathrm{IVEV}(i) P_i \qquad [4]$$

In addition to the aIVEV, the *Individual Required Safe Egress Time* (IRSET) for each device is considered to aid in deciding the vulnerability of areas of the geometry. That is, the total egress time (from alarm activation to escape) for the assistance device from that location if evacuating on its own. Let the IRSET for hazard i be denoted $\mathrm{IRSET}(i) = T(i) + Prep. + Resp.$ where "$Prep.$" is the preparation time for the device and "$Resp.$" is the longest possible response time of staff. This value provides a useful benchmark to show the longest RSET possible for the device from the location in the absence of interactions with other evacuating occupants. The actual longest RSET experienced in a full building evacuation will likely be greater than this. The *maximum Individual Required Safe Egress Time* (mIRSET), representing the maximum IRSET from the location over all the scenarios, is obtained from Equation [5].

$$\mathrm{mIRSET} = \max_{i=0,\dots,n} (\mathrm{IRSET}(i)) \qquad [5]$$

Results Interpretation

To determine the distribution of patients throughout the hospital, both the aIVEV and the mIRSET are considered. No patient should be placed in an area whose mIRSET for the assistance device they require is greater than the ASET for a predicted scenario. In addition, patients should not be placed in an area with an aIVEV of more than the egress time weighting w_T. This is because, if aIVEV $\geq w_T$, then this location is at least as vulnerable as a location with the smallest dimensionless spaciousness and isovist ($\hat{S} = 0$ and $\hat{I} = 0$) and the largest dimensionless egress time ($\hat{T} = 1$). When this is the case, the mIRSET will be greater than the ASET. Therefore, if aIVEV $\geq w_T$, the location is at least as vulnerable as a location where the mIRSET is greater than the ASET. As a result, the actual mIRSET of the location may be beyond the mIRSET predicted by HEPTAD. This could be because it is difficult to manoeuvre the device into the area (low spaciousness) or for staff to notice the patient (low isovist); increasing the response time. For each device, areas of the geometry are colour coded to produce *risk zones* using the following heuristic:

- Areas with mIRSET $\geq$ ASET are marked as red risk zones: patients requiring this device should never be placed in these areas.
- Areas that are not red risk zones but with aIVEV $\geq w_T$ are marked as amber risk zones: patients requiring this device should not be placed in these areas. However, these zones can be upgraded to green risk zones if measures are put in place to improve the visibility of the patient (to increase the isovist) and/or provide a clearer path for the device to enter and exit the zone (to increase the spaciousness).
- All areas that are not red or amber risk zones are marked as green risk zones: patients requiring this device should, where possible, be allocated beds in these risk zones.

Within these zones, areas with a lower mIRSET and aIVEV scores should be prioritised and further analysis may be required to take into account other evacuating people.

Note that HEPTAD does not currently take into account the impact of other occupants during the evacuation in its calculation of risk zones. Thus, while HEPTAD can be used to identify inappropriate areas for a particular patient, it cannot alone be used to determine the appropriate areas that can be evacuated within a given ASET. In other words, all appropriate areas will lie within green risk zones but not all green risk zones are appropriate areas. To determine which areas in green risk zones are appropriate, further analysis is required that takes into account the impact of other occupants during the evacuation in addition to the aIVEV and mIRSET values from HEPTAD. The impact of other occupants during the evacuation will be represented when HEPTAD is incorporated into the EXODUS egress model.

TEST CASE

To demonstrate the functionality of HEPTAD, a test case of a hypothetical hospital layout was constructed along with several scenarios. Only the ground floor of the building was considered as HEPTAD does not yet have the functionality to include stairways. The floor plan is shown in Figure 7. The usable space in this geometry was input into HEPTAD with 16 rooms (R1-16), 4 external exits (E1-4) and an internal exit (E5). The hypothetical layout is based on a hospital geometry that was in use up to 1986. As such, many of the doorways are not code compliant [7,21] by modern standards as they have an effective width of only 1000mm. However, code-compliant evacuation routes do exist from R3, R8, R9, R10 and the main corridor. This mix of compliant and non-compliant areas of the geometry is designed to test HEPTAD's ability to determine viable evacuation routes in both areas for different assistance devices and show the effect compliancy has for different devices.

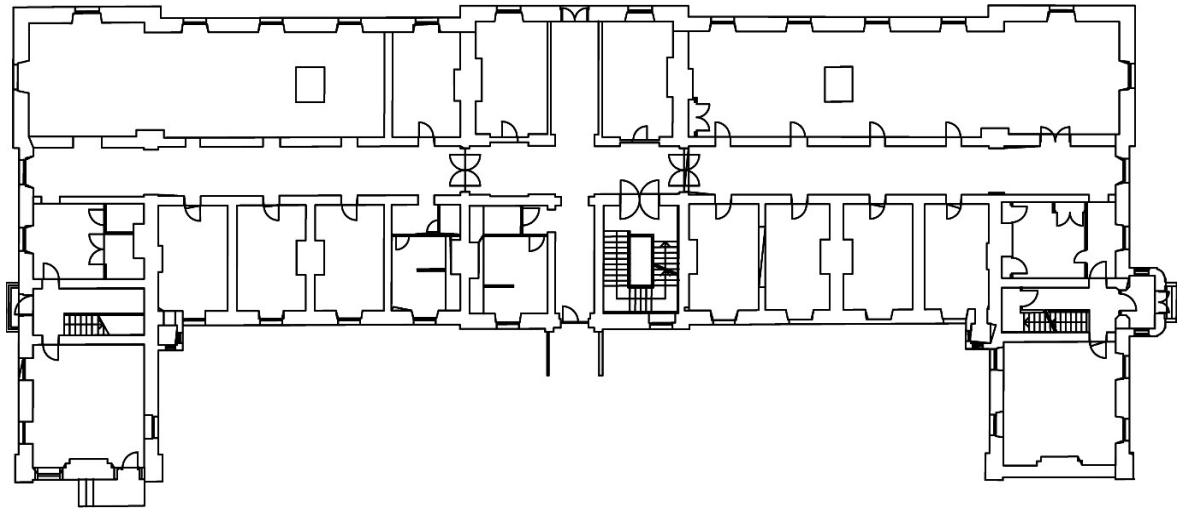

Figure 7: Hypothetical geometry used in the test case.

Three hazards were added to the geometry each with its probability of being active during an evacuation. Two of these hazards were added at either end of the geometry blocking main exists

and one in the middle blocking the main corridor. These locations were chosen to demonstrate the impact each hazard has on its surrounding area. For the scenarios represented by the hazards, an ASET of 150 seconds and a response time of 50 seconds were assumed. These scenarios were selected for demonstration purposes only. The hazards and room labelling are shown in Figure 8 and the hazard information is shown in Table 1.

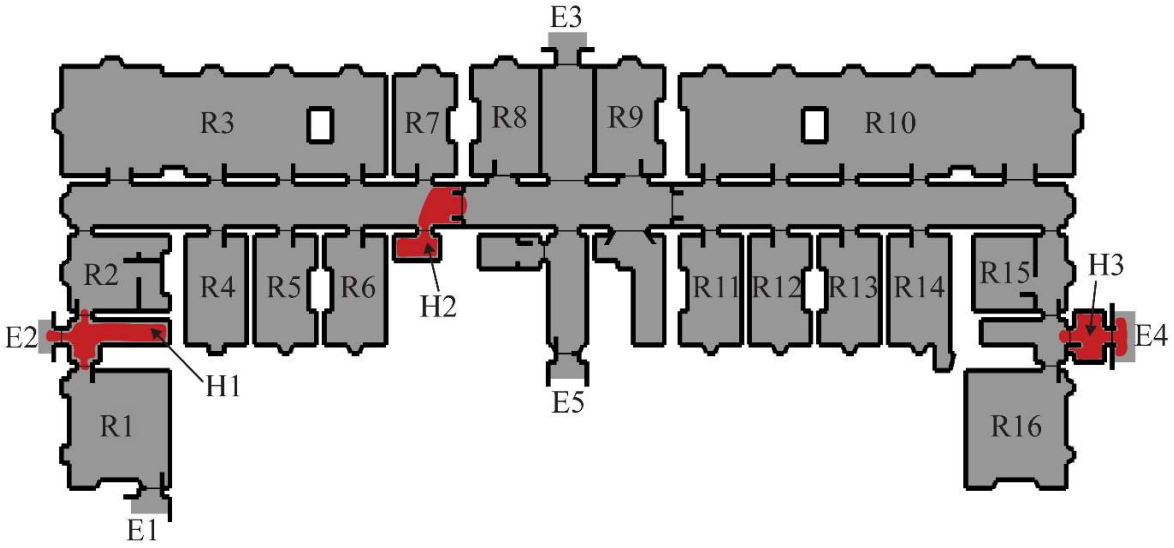

Figure 8: Geometry represented in HEPTAD with rooms (R1-16), exits (E1-5) and hazards (red) (H1-3).

Hazard	**Scenario**	**Probability Active During Evacuation [%]**	**Floor area disrupted [m^2]**
0	No hazard.	22	0.0
1	Fire between R1 and R2 blocking E2.	33	15.25
2	Fire in storage cupboard to the right of R6 blocking the main corridor.	25	11.0
3	Fire in storage cupboard next to E4 blocking this exit.	20	10.25

Table 1: Scenario, probability and size of each hazard.

Within this geometry and set of scenarios, three different assistance devices were compared. These were an Evacuation Chair (EC), Rescue Sheet (RS) and Hospital Bed (HB). Most of the parameters for these devices were either taken directly from data collected by Adams & Galea [3,8,9] and Hoondert et al [27] or inferred from these data. However, due to a lack of available data, the rest were estimated based on video footage and photographs. As such, these parameters, presented in Table 2, are for demonstration purposes only. A photograph of each device along with its 2D representation in HEPTAD is shown in Figure 9.

Property	Evacuation Chair	Rescue Sheet	Hospital Bed
Max linear speed $[m/s]$	1.54 [3,8]	1.38 [3,8]	1.23 [27]
Max angular speed $[°/s]$	163.3 [3,8] †	49.3 [3,8] †	22.5 ‡
Acceleration rate $[m/s^2]$	0.4 ‡	0.5 ‡	0.4 ‡
Holonomicity	Non-holonomic ‡	Non-holonomic ‡	Holonomic ‡
Min turning radius $[m]$	0.0 ‡	0.0 ‡	0.0 ‡
Preparation time $[s]$	29 [3,8]	53 [3,8]	31 [27]
Length (excluding attendants) $[m]$	0.77 [3,9]	2.00 [3,9]	2.18 ‡
Width (excluding attendants) $[m]$	0.52 [3,9]	0.75 [3,9]	0.92 ‡
Number and position of attendants	1 at back (fixed) [3,8]	2 at front (fixed) [3,8]	1 at back (fixed) and 1 at front (able to move around device) [27] †

Table 2: Properties of devices (for demonstration purposes only) – † value inferred from data in reference; ‡ value estimated through observations of video footage and photographs.

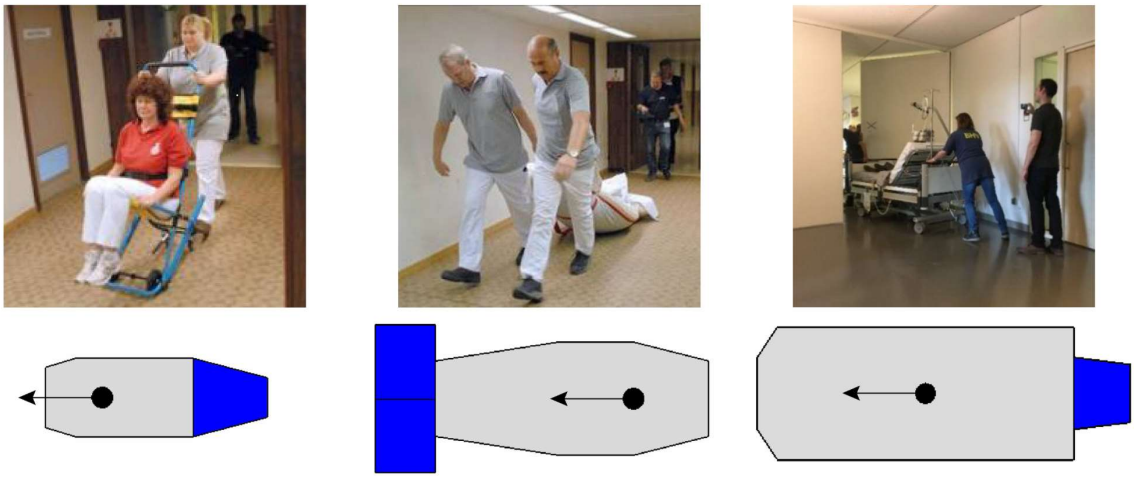

(a) Evacuation Device (b) Rescue Sheet (c) Hospital Bed

Figure 9: Photographs [9,27] and corresponding 2D representations of the assistance devices. Blue area(s) denote attendant(s), grey area denotes the device and arrow shows forward direction.

RESULTS

Base Case (No Hazards)

The building geometry was input into HEPTAD along with the properties of the assistance devices. The value of isovist, spaciousness, egress time and IVEV were collected for each $0.25m \times 0.25m$ cell in the geometry. For the scenario with hazard 0 (no hazards), the isovist

for the geometry is presented in Figure 10 and spaciousness for each device are presented in Figure 11 (EC), Figure 12 (RS) and Figure 13 (HB) as heat maps. The average IRSET and IVEV values for each room are presented as bar charts in Figure 14.

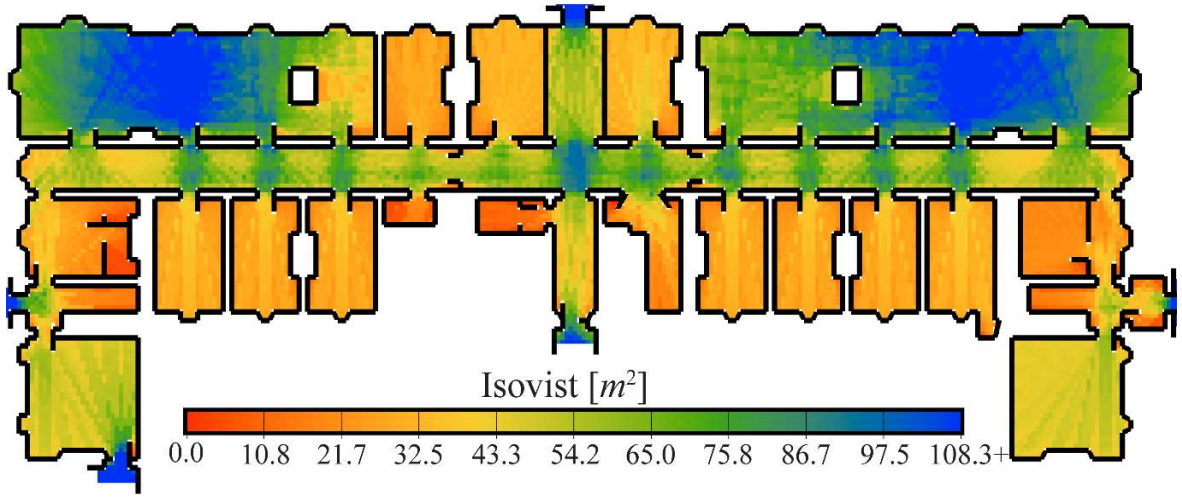

Figure 10: The isovist for the geometry.

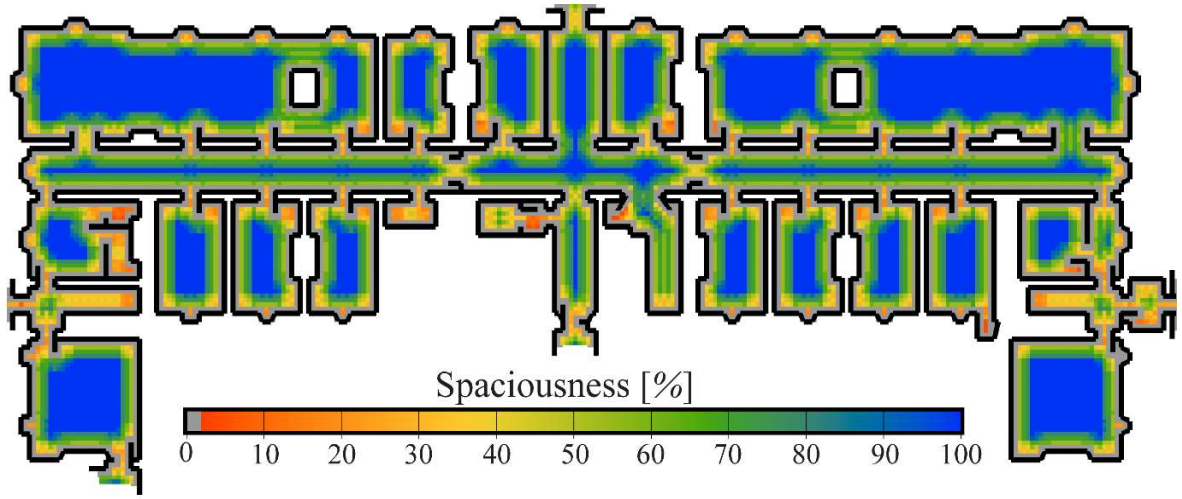

Figure 11: The spaciousness for EC.

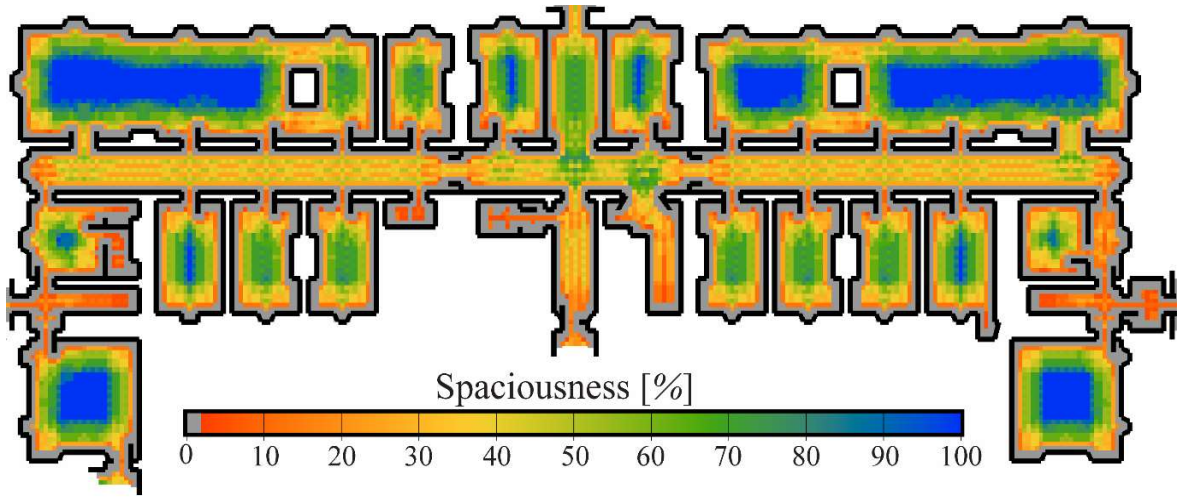

Figure 12: The spaciousness for RS.

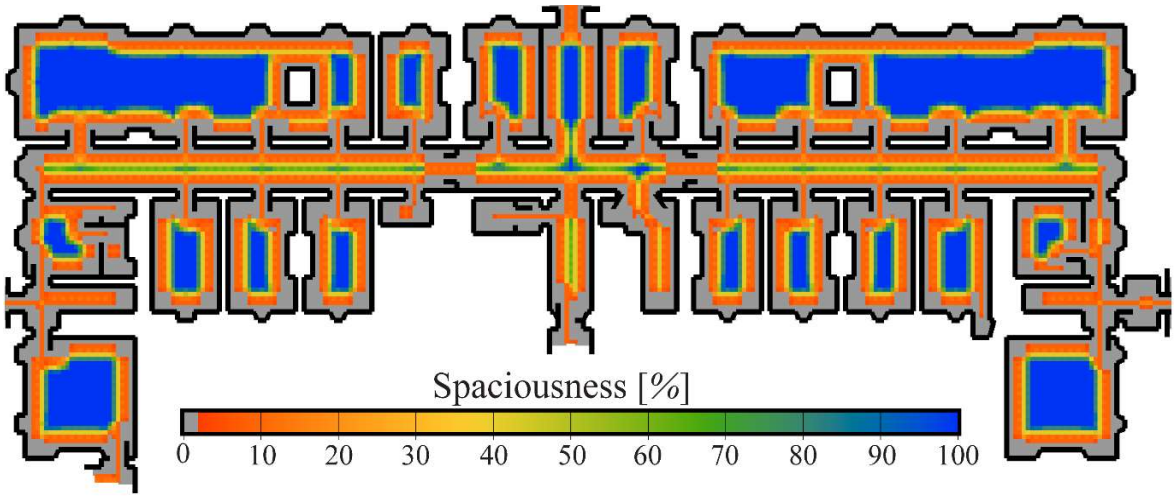

Figure 13: The spaciousness for HB.

The isovist and spaciousness values were found to be lower near the perimeter of rooms as boundary lines obstruct the assistance device and reduce the visibility of surrounding areas. These values were also generally lower in smaller or narrower areas such as corridors or small rooms. This results in an increase in IVEV in smaller or narrower areas and near boundaries.

The data collected from HEPTAD suggested that the EC performed better than the RS and HB for all factors (spaciousness, egress time, IRSET and IVEV) for all rooms. This was not surprising when considering the EC's smaller size, larger linear and angular speeds and shorter preparation time compared to the other devices. The RS had a lower egress time than the HB for most rooms despite being a non-holonomic device while the HB was holonomic. This was likely due to the slightly smaller size and faster linear and angular speeds. However, when considering the IRSET and IVEV, the HB performed better in most rooms. This was due to the relatively short preparation time experienced by the HB compared to the RS (22 seconds shorter).

It can be seen from Figure 14 that the RS and HB had a relatively long egress time for rooms R15 and R16 while the EC had a relatively short egress time. This was because, unlike the EC, the RS and HB could not manoeuvre through the small gap next to E4 so had to use a different exit. This difference in viable routes was reiterated when looking at the egress route taken by all three devices from the same configuration in the top right of the geometry (R10) as shown in Figure 15. The routes from this location had an egress time of 18 seconds for the EC, 42 seconds for the RS and 52 seconds for the HB. This difference is partly due to the EC exiting through E5 while the RS and HB exited through E3 giving a much longer egress route from the same location. In addition, the RS and HB used a different door to exit R10, the RS utilising a code-compliant [7,21] doorway (width 2000mm) and the HB utilising a non-compliant doorway (width 1000mm). This highlights the potential difference in available routes for holonomic and non-holonomic assistance devices.

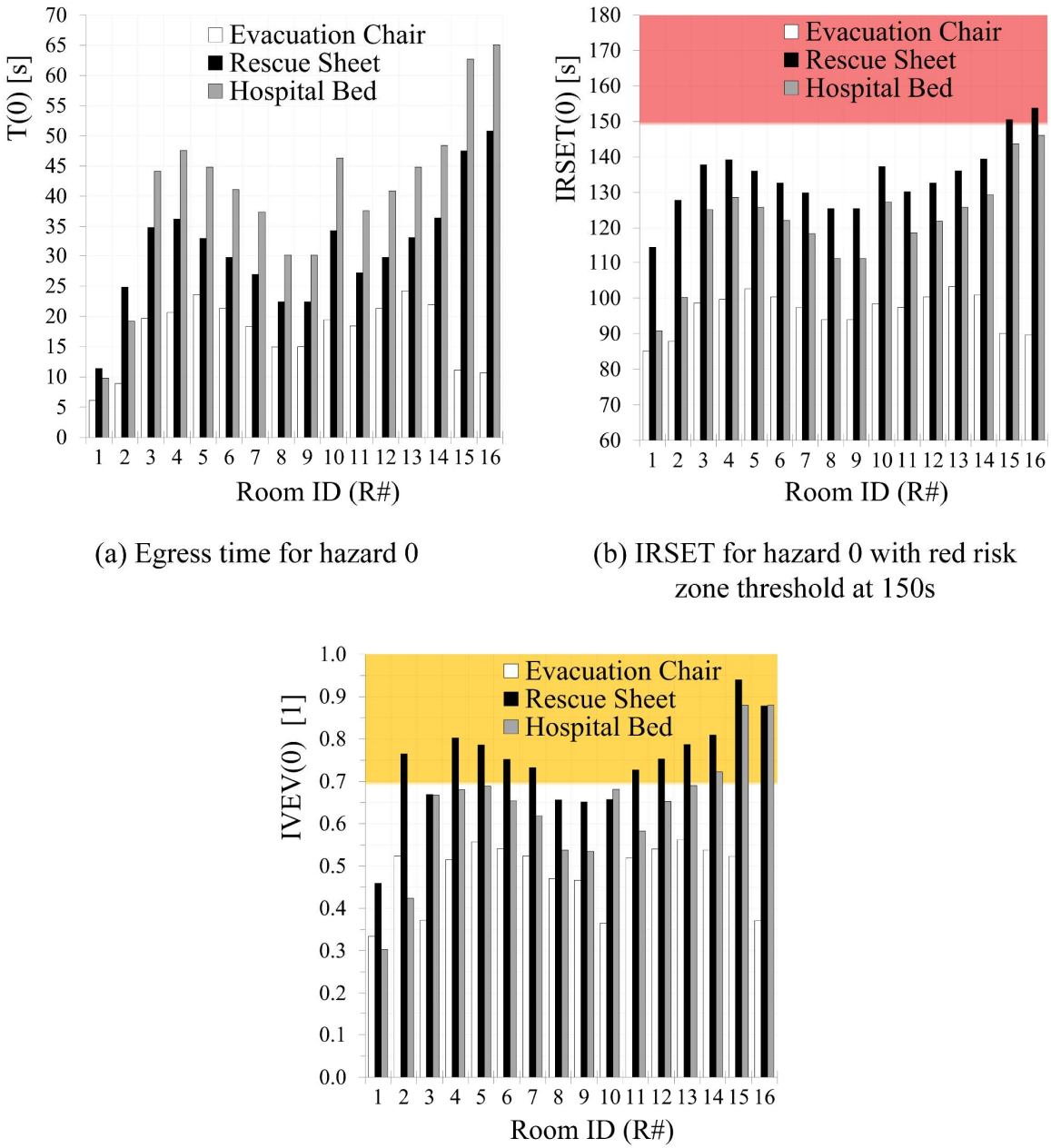

(a) Egress time for hazard 0

(b) IRSET for hazard 0 with red risk zone threshold at 150s

(c) IVEV for hazard 0 with amber risk zone threshold at 0.7

Figure 14: Egress time, IRSET and IVEV for all three devices for hazard 0 (no hazards).

Based on the values produced by HEPTAD (determined by the thresholds in Figure 14), all 16 rooms were green risk zones for a patient requiring an EC compared to 13 for a HB and only 5 rooms for a RS. The number of red, amber and green risk zones differed, however, when hazards were considered.

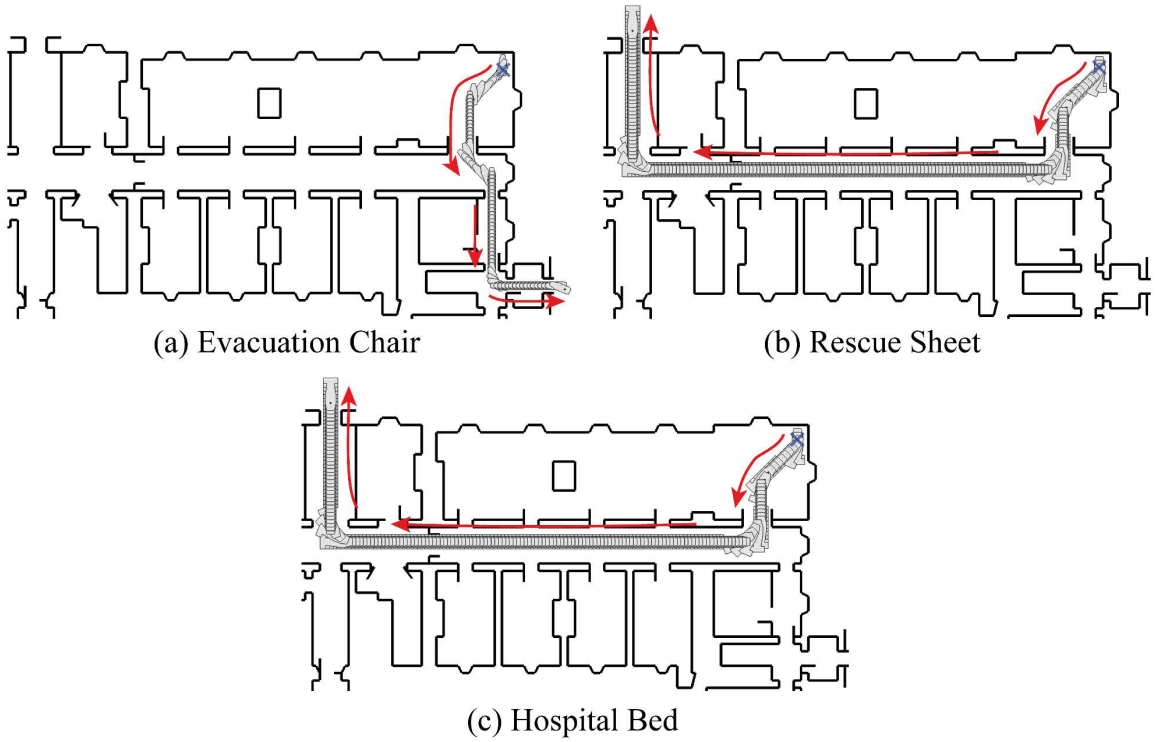

Figure 15: Egress routes from same start configuration (top right of geometry facing south) of the evacuation chair, rescue sheet and hospital bed. Start position marked with blue cross, device position and orientation along the route shown as onion skinning of its shape in grey and direction of the route marked with red arrows.

Effect of Hazards

For each hazard entered into HEPTAD, egress routes from every location were recalculated giving different egress times and IVEVs. If a base case route travelled through a hazard, the route of the assistance device was altered to avoid the hazard which may have caused it to use an alternative exit. The effects of each hazard on the IVEVs are shown in Figure 16.

From Figure 16, hazard 1 affected R1, R2, R3, R4 and R5. Averaged over the devices, the increase in IVEV for these rooms was 0.004, 0.232, 0.039, 0.018 and 0.002 respectively. From these values, it can be seen that the effect on R2 is much larger than that on the other rooms. This was likely due to the proximity of the hazard to this room and the large distance from this room to the next nearest available exit (E3 or E5). Likewise, hazard 2 had the largest effect on the IVEVs of R7 and hazard 3 had the largest effect on the IVEVs of R16.

As well as increasing the distance to a viable exit, hazards were also seen to trap devices in a room (giving infinite egress time). In this test case, the HB was the only device trapped by a hazard. This was because its larger size reduced its ability to manoeuvre around hazards, increasing the probability of a trap occurring. These traps occurred in R7 when hazard 2 was active and R16 when hazard 3 was active. The trapping in R7 can be seen in Figure 16 by the increase in IVEV (of 0.322) for R7 by hazard 1. However, Figure 16 shows only a small increase in IVEV (of 0.042) for R16 by hazard 3. This small increase is because of the already

high IVEV for the HB in that room (0.880) in the base case caused by its inability to use E4.

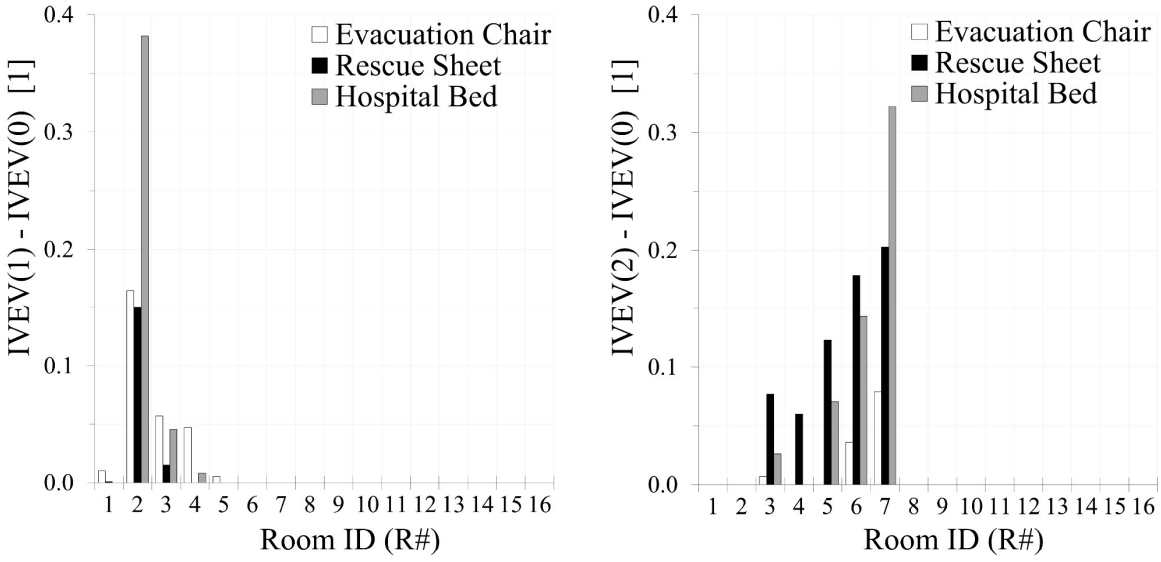

(a) Increase in IVEV caused by hazard 1

(b) Increase in IVEV caused by hazard 2

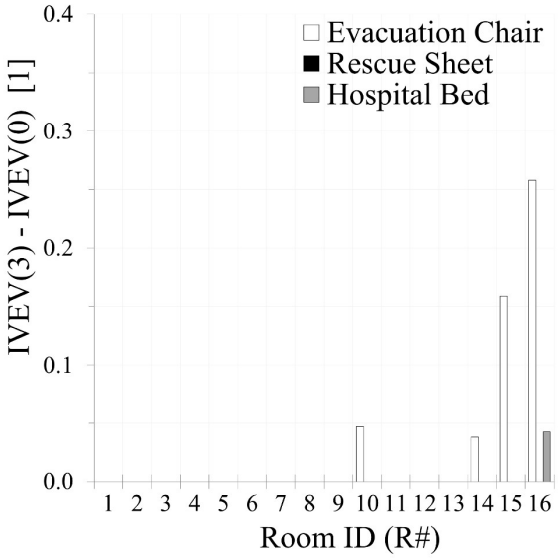

(c) Increase in IVEV caused by hazard 3

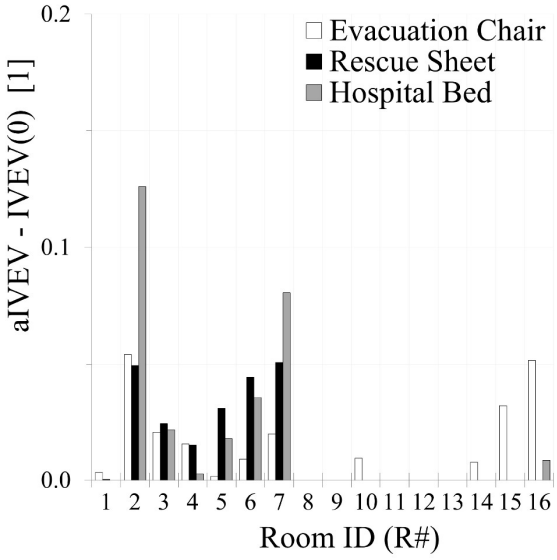

(c) Weighted (by probability) average increase in IVEV

Figure 16: Bar charts showing the difference between IVEV with no hazard (IVEV(0)) and IVEV with hazard n active (IVEV(n)) for each room and each device.

Hazards 1 and 2 had little effect on the IVEV of the EC when compared to the other devices. This was because the alternative routes from R1, R2, R3, R4, R5, R6 and R7 could be traversed by the EC in less time due to its faster linear and angular speed. By contrast, hazard 3 had the biggest effect on the IVEV of the EC compared to the other devices. This hazard blocked the

nearest available exit, E4, forcing the EC to find an alternative route from R10, R14, R15 and R16. Since E4 was unusable for the RS and HB in the absence of hazards, alternative routes did not need to be found and the IVEVs of these devices were not affected (other than the aforementioned trapping of the HB in R16). An example of the route alteration for the EC as a result of hazard 3 can be seen in Figure 17 when compared to the route taken from the same location in the base case in Figure 15. This hazard increased the egress time for the EC from the location in Figure 15 by 75%. As the next nearest exit, E3, was much farther from the affected rooms, the alternative routes were much longer than routes in the base case.

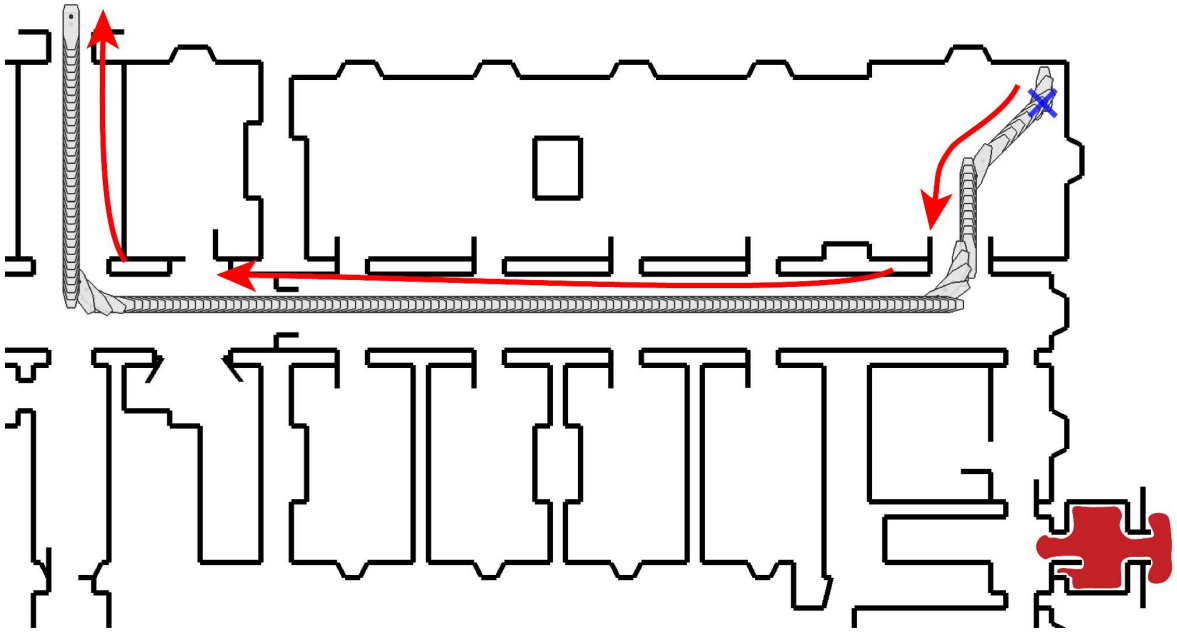

Figure 17: Egress route taken by EC from the top right of the geometry differs from that in Figure 15 when hazard 3 is active.

To determine the risk zones for each room for each device, the mIRSET and aIVEV were calculated. These values with the corresponding risk zone thresholds are given in Figure 18. The results obtained from HEPTAD suggested that all 16 rooms were identified as green risk zones for a patient requiring the use of an EC. By contrast, only 5 rooms were identified as green risk zones for the RS (R1, R3, R8, R9 and R10) and 11 rooms were green risk zones for the HB (R1, R2, R3, R4, R6, R8, R9, R10, R11, R12 and R13). The risk zone colouring for the devices are given in Figure 19 (EC), Figure 20 (RS) and Figure 21 (HB). Based on these colourings, hospital or ward managers should not place patients who require the use of a device in the red risk zones for that device. This means that bedridden patients who cannot be transferred to another assistance device must be placed in the green risk zones for the HB. Further analysis would be required to take into account other evacuating populations before a distribution of these patients in the green risk zones can be determined.

During full evacuations of large multi-storey hospitals, patients on higher floors will have to be taken down several stories to reach an external exit. The HB will likely perform much worse than vertical assistance devices in these scenarios as it cannot be taken down stairways and lifts must be used where available. This would greatly increase the egress time for a HB, particularly in the event of a lift failure. The Health Technical Memorandum 05-02 [7] states that these events

should only occur "if a fire cannot be controlled within the space of origin and there is additional risk to occupants outside of the fire compartment of origin" and are therefore very rare. However, bedridden patients on higher floors may have a significant risk of not evacuating within the ASET if a full evacuation were to occur. Restricting bedridden patients to the ground floor (or a floor with an external exit) would reduce their vulnerability in these situations.

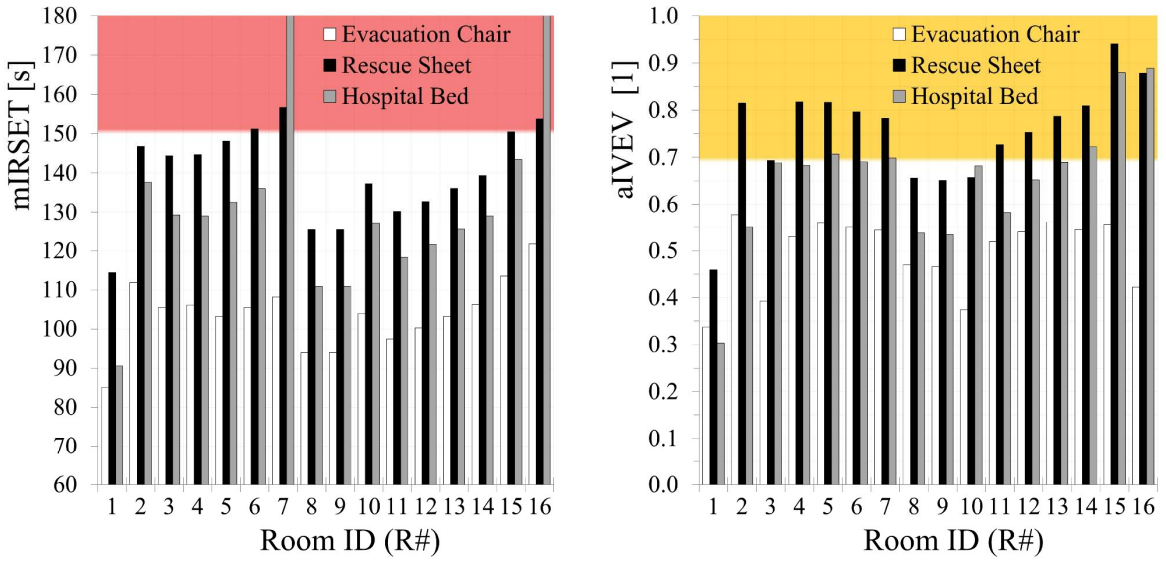

(a) mIRSET with red risk zone threshold at 150s

(b) aIVEV with amber risk zone threshold at 0.7

Figure 18: Bar charts showing the mIRSET and aIVEV values for each room and each device.

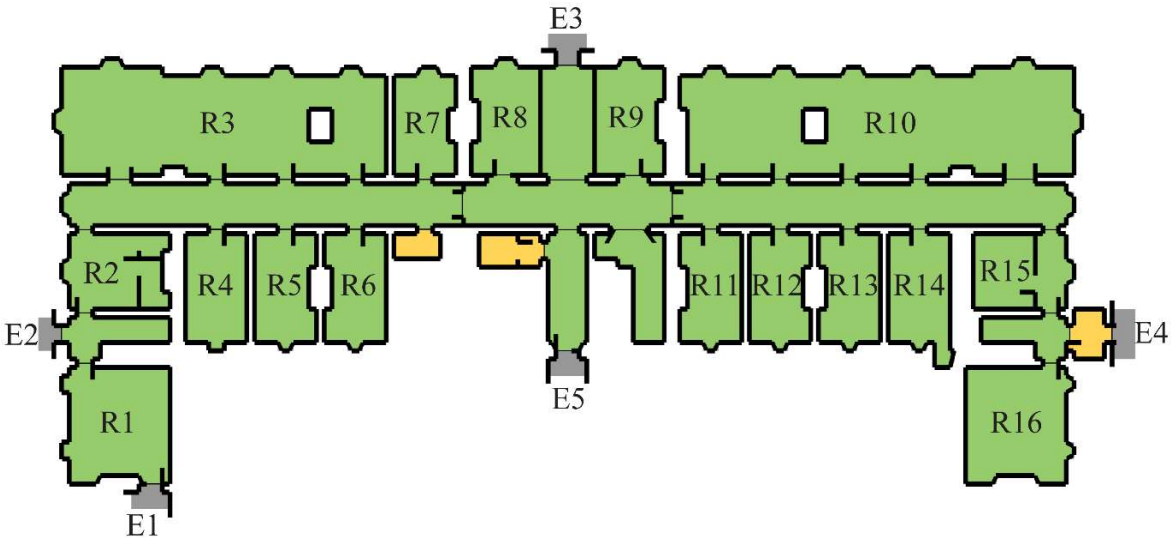

Figure 19: Risk zone colouring for the EC.

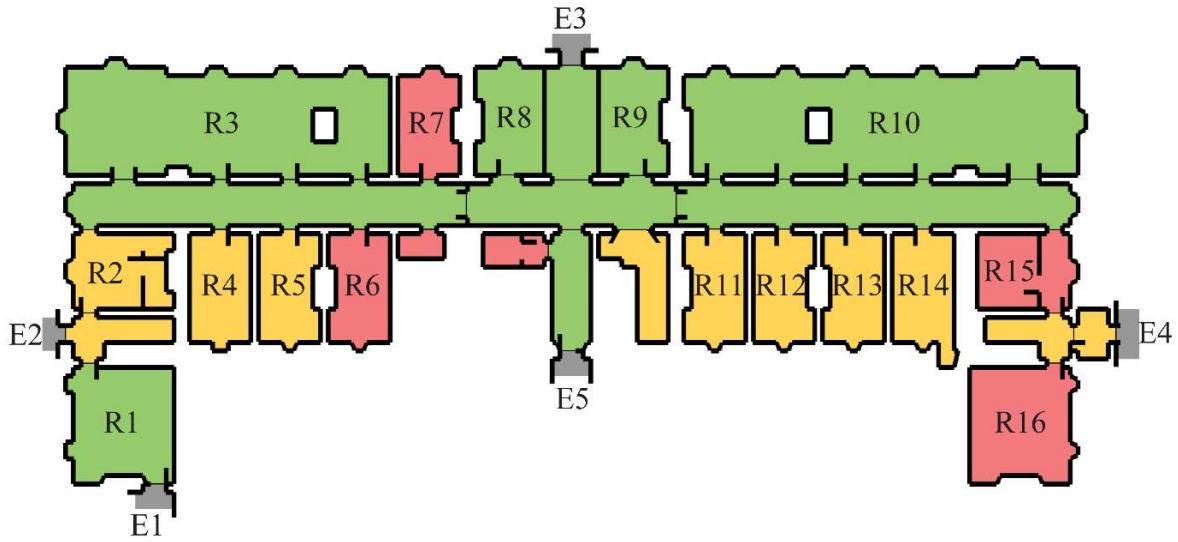

Figure 20: Risk zone colouring for the RS.

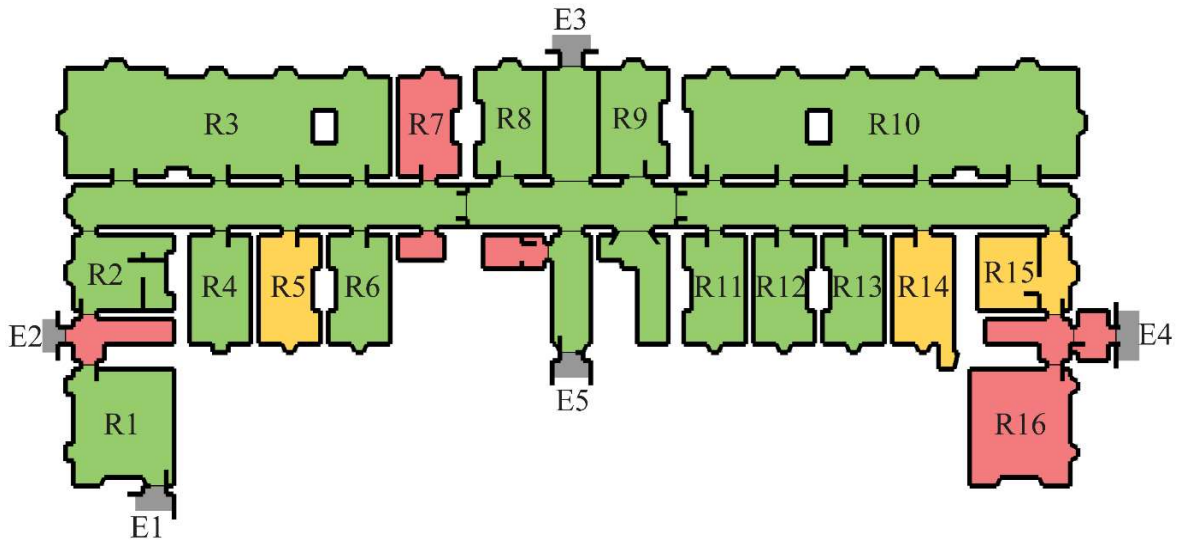

Figure 21: Risk zone colouring for the HB.

For the base case, the egress time and IVEV for all devices were lower in rooms nearer exits, which was as expected. Also, larger rooms tended to have a lower IVEV than smaller rooms with a similar egress time. This was due to the larger spaciousness and isovist values. When hazards were introduced, the mIRSET and aIVEV of both devices increased for rooms that were both near the hazard and where the hazard was between the room and the nearest exit. In addition, larger devices generally gave smaller spaciousness values and the more constrained a device (spatially or kinematically) the larger the egress time. Hence, the model predictions for this simple example were in line with informed expectations.

DISCUSSION AND RECOMMENDATIONS

The test case demonstrates that HEPTAD can estimate the egress time of assistance devices from each location in the geometry in the absence of other moving entities by finding viable routes based on their spatial and kinematic constraints. Using these results, the tool can also

determine the areas of the geometry that are inappropriate for patients with specific mobility requirements (red and amber risk zones). Since the risk zones produced by HEPTAD currently do not take into account other evacuating occupants, they should not alone be used to determine a distribution of patients throughout a hospital that meets the ASET requirements. Although patients should be restricted to green risk zones, as currently HEPTAD does not take into consideration the impact of other occupants during the evacuation, the results from HEPTAD should be used in combination with other methods (such as hand calculation tools or evacuation simulation models) to determine the most appropriate areas within these zones to accommodate patients with specific mobility requirements.

The test case also demonstrates that patients who require different assistance devices experience a different level of risk for the same room and scenario. This is due to the different spatial and kinematic constraints of devices which influence the available viable egress routes for each device. This difference in routes, as seen in Figure 15, highlights the importance of accurately representing these constraints as routes that are available to some devices will not be available to others. This becomes even clearer when considering that an exit (E4) was inaccessible to the RS and HB but accessible to the EC despite the exit failing to meet code compliance [7,21]. This difference in accessibility is consistent with research concerning the Royal Marsden hospital evacuation where it was found that staff utilising rescue sheets had difficulty manoeuvring the devices through noncompliant doorways [2]. Compliant evacuation routes within a hospital geometry are likely (though not guaranteed) to be accessible to any assistance device. This is evidenced by HEPTAD producing green risk zones for all devices in R3, R8, R9, R10 and the main corridor. These are the only areas in the geometry that have compliant evacuation routes. This difference in accessibility shows that HEPTAD can detect viable yet incompliant evacuation routes within a geometry that would currently be avoided by assistance devices. Furthermore, HEPTAD can be used to identify viable egress routes for assistance devices in other building types that may be subject to less restrictive building code requirements.

Kinematic constraints of assistance devices affect the way in which they can follow a viable route. For example, in Figure 15, the HB (a holonomic device) moves through R10 without rotating and only rotates once it reaches the corridor. This contrasts the movement of the other (non-holonomic) devices from the same room and may explain why HEPTAD predicted that the HB would use a different door to the RS when leaving R10 for the same exit. HEPTAD highlights that a less spatially and kinematically constrained device will generally perform better in an evacuation.

When hazards are incorporated, the IVEV of a room is only affected if a device passes through the location of the hazard while following the egress route from that room in the base case. This means that each hazard has the largest influence on the IVEVs of nearby rooms and this influence depends on the length of an alternative route. Areas near an exit are, generally, the farthest from an alternative exit. This means if an exit is blocked by a hazard, the areas near this exit will experience the greatest increase in egress time and, therefore, IVEV.

As a result of the research carried out in this paper, the following recommendations are made for various stakeholders involved in evacuation management:

- For Hospital Emergency Coordinators (HECs): To improve evacuation efficiency, careful consideration should be given to the allocation of patients to rooms. This must

take into consideration the patients' mobility requirements to ensure that an evacuation using the appropriate assistance device is feasible from their location. In addition, both primary and alternative evacuation routes must be determined for each patient using an appropriate device.

- For assistance device manufacturers: Design goals should be to maximise the manoeuvrability of the device by minimising its constraints. This can be by ensuring there is no minimum turning radius (it can turn on the spot) and it is holonomic (the possible directions of movement do not depend on the direction it is facing) as well as reducing the size as much as possible with no protrusions that may hinder its movement. In addition, more details about the performance of the device should be provided (such as in Table 2) by carrying out independent studies with different demographics of participants.
- For egress model developers: Incorporate the relevant spatial and kinematic constraints of assistance devices (and other objects) into simulation models as these influence the movement of devices and the movement of others who are evacuating with devices.

Although HEPTAD is designed primarily for use in hospitals, it can be applied to any building that utilises assistance devices. This is particularly useful for determining egress routes through buildings types with less restrictive building codes such as residential buildings and office blocks. In addition, any moveable object whose properties can be empirically established (as in Table 2), such as vehicles, luggage, and moveable furniture, can be represented using the methods presented here. The tool can also be used to test and identify potential issues with new concept assistance devices for application in existing hospital buildings once the properties of the device can be established. It is hoped that the methods used here will enable egress model developers to extend the capabilities of their models to include any moveable object that may be applicable in different scenarios and geometries.

CONCLUSIONS AND FUTURE WORK

This research has demonstrated that the spatial constraints (size and shape) and kinematic constraints (maximum speeds, turning radius and holonomicity) of movement assistance devices may adversely impact the viability of certain egress routes in a hospital geometry. These constraints potentially limit evacuation options and, as a result, increase egress times associated with devices. Despite this, current egress models have been unable to represent many of the constraints of movement assistance devices and therefore are likely to produce over-optimistic qualitative and quantitative predictions. The HEPTAD software has represented a step forward in the development of egress models by demonstrating how these constraints could be incorporated utilising methods from fields of study outside of fire safety engineering (primarily autonomous robotics).

As well as demonstrating the functionality of the theoretical models, HEPTAD itself can be used by Hospital Emergency Coordinators (HECs) to aid in evacuation planning, staff training and live route-finding during real evacuations. HEPTAD can do this by identifying viable routes for movement assistance devices throughout an arbitrarily complex building layout while taking into account the device constraints. In addition, the software can classify areas of the hospital geometry into risk zones without the need to run separate simulations of the movement of such devices from every start location. These risk zones provide information to

HECs that can be utilised during the design phase of building construction or when deciding on the positioning of different wards within an existing hospital building. This enables HECs to take into account the selection of movement assistance devices that are appropriate for the mobility requirements of each patient that may occupy a ward. This may reduce the risk of allocating patients to beds from which they cannot be evacuated within a safe egress time.

Future work is needed to incorporate stairways into the model and increase the number of movement directions from 8 to 16 allowing for a finer fidelity in the movement of assistance devices. In addition, an ability to represent the interactions between movement assistance devices and other occupants is underdevelopment. Once this new capability is developed, HEPTAD will be merged with the EXODUS egress model allowing the combined software to represent the interaction of arbitrary moveable objects such as assistance devices, vehicles and luggage within the general evacuation flow. Although these methods could also be utilised to represent moveable obstacles, such as debris and furniture, further research is needed to determine how occupants interact with these obstacles during an evacuation to allow for a representation of a dynamic geometry in simulation models.

ACKNOWLEDGEMENTS

Michael Joyce would like to thank the University of Greenwich for funding his VC Scholarship and FSEG for the opportunity to participate in this research.

REFERENCES

1. Home Office. *FIRE STATISTICS TABLE 0301*. London: Home Office; 2018. www.gov.uk/government/statistical-data-sets/fire-statistics-data-tables. Accessed November 13, 2019.
2. Wapling A, Heggie C, Murray V, Bagaria J, Philpott C. *Review of Five London Hospital Fires and Their Management*. London; 2009.
3. Adams APM, Galea ER. An Experimental Evaluation of Movement Devices Used to Assist People with Reduced Mobility in High-Rise Building Evacuations. In: Peacock, R.D., Kuligowski, E.D., and Averill JD, ed. *Pedestrian and Evacuation Dynamics*. Maryland: Springer, New York; 2010:130-138. doi:10.1007/978-1-4419-9725-8
4. Yanagawa Y, Kondo H, Okawa T, Ochi F. Lessons learned from the total evacuation of a hospital after the 2016 Kumamoto Earthquake. *J Emerg Manag*. 2017;15(4):259-263. doi:10.5055/jem.2017.0334
5. Catovic L, Alniemi C, Ronchi E. A survey on the factors affecting horizontal assisted evacuation in hospitals. In: *3rd European Symposium on Fire Safety Science 12–14 September 2018*. Vol 1107. Journal of Physics: Conference Series. IOP Publishing; 2018:072001. doi:10.1088/1742-6596/1107/7/072001
6. Wabo NC, Örtenwall P, Khorram-Manesh A. Hospital evacuation; planning, assessment, performance and evaluation. *J Acute Dis*. 2012;1(1):58-64. doi:10.1016/S2221-6189(13)60056-6
7. Department of Health. *Health Technical Memorandum 05-02: Firecode*.; 2015. https://assets.publishing.service.gov.uk/government/uploads/system/uploads/attachment_data/file/473012/HTM_05-02_2015.pdf.

8. Hunt A, Galea ER, Lawrence PJ. An analysis and numerical simulation of the performance of trained hospital staff using movement assist devices to evacuate people with reduced mobility. *Fire Mater*. 2013;39(4):407-429. doi:10.1002/fam.2215
9. Hunt A. Simulating Hospital Evacuation. *[PhD thesis] Univ Greenwich*. 2016.
10. Cooper LY. A concept for estimating available safe egress time in fires. *Fire Saf J*. 1983;5(2):135-144. doi:10.1016/0379-7112(83)90006-1
11. Wang C, Savkin A V., Clout R, Nguyen HT. An intelligent robotic hospital bed for safe transportation of critical neurosurgery patients along crowded hospital corridors. *IEEE Trans Neural Syst Rehabil Eng*. 2015;23(5):744-754. doi:10.1109/TNSRE.2014.2347377
12. Matveev AS, Savkin A V., Hoy M, Wang C. Biologically-inspired algorithm for safe navigation of a wheeled robot among moving obstacles. In: *Safe Robot Navigation Among Moving and Steady Obstacles*. Butterworth-Heinemann; 2016:161-184. doi:10.1016/b978-0-12-803730-0.00008-1
13. Tecdron Robotic Systems. TC800-FF Technical assistance and fire-fighting robot. www.robotpompier.com/en/. Published 2018. Accessed September 30, 2019.
14. Galea ER, Lawrence PJ, Gwynne S, Filippidis L, Blackshields D, Cooney D. *BuildingEXODUS v6.1 THEORY MANUAL*. London: University of Greenwich; 2014.
15. Florida Department of Health. *Hospital Emergency Evacuation Toolkit*.; 2011. www.floridahealth.gov/programs-and-services/emergency-preparedness-and-response/disaster-response-resources/discharge-planning/_documents/ evac-toolkit.pdf.
16. Childers A, Taaffe K. Healthcare Facility Evacuations: Lessons Learned, Research Activity, and the Need for Engineering Contributions. *J Healthc Eng*. 2010;1(1):125-140. doi:10.1260/2040-2295.1.1.125
17. Ünlü A, Ülken G, Edgü E. A Space Syntax Based Model in Evacuation of Hospitals. In: *Proceedings, 5th International Space Syntax Symposium*. Delft, Holland: Space Syntax Laboratory; 2005:161-171. http://spacesyntax.tudelft.nl/media/longpapers2/alperunlu.pdf.
18. Hashemi M. Dynamic, Stream-Balancing, Turn-Minimizing, Accessible Wayfinding for Emergency Evacuation of People Who Use a Wheelchair. *Fire Technol*. 2018;54(5):1195-1217. doi:10.1007/s10694-018-0735-x
19. Dijkstra EW. A Note on Two Problems in Connexion with Graphs. *Numer Math*. 1959;1:269-271. doi:10.1007/BF01386390
20. United States Department of Homeland Security. *Responder Assessment and Validation of User Equipment (RAVUE): Non-Motorized Extrication Devices*.; 2004. https://www.hsdl.org/?view&did=452304.
21. Department of Health. *Health Building Note 00-04: Circulation and Communication Spaces*.; 2013. https://www.gov.uk/government/uploads/system/uploads/attachment_data/file/187026/Health_Building_Note_00-04_-_Circulation_and_communication_spaces_-_updated_April_2013.pdf.
22. Siegwart R, Nourbakhsh IR, Scaramuzza D. *Introduction to Autonomous Mobile Robots*. 2nd ed. Cambridge: Massachusetts Institute of Technology; 2011.
23. Thunderhead Engineering. *Pathfinder Technical Reference*. Manhattan: Thunderhead Engineering; 2017. www.thunderheadeng.com/pathfinder/resources. Accessed October 15, 2018.
24. Ronchi E, Corbetta A, Galea E, Kinateder M, Kuligowski E, McGrath D, Pel A, Shiban Y, Thompson P, Toschi F. *New Approaches to Evacuation Modelling*. (Ronchi E, ed.).

Lund: Lund University, Department of Fire Safety Engineering; 2017.
25. Wall DJG. A Graph-Theory-Based C-Space Path Planner for Mobile Robotic Manipulators in Close-Proximity Environments. *[PhD thesis] Cranf Univ*. 2016.
26. Vaidya SK, Kanani KK, Vihol PL, Dani NA. Some cordial graphs in the context of barycentric subdivision. *Int J Contemp Math Sci*. 2009;4(29-32):1479-1492.
27. Hoondert P, Peters B. New Design Approach for Fire Safe Hospital Wards. In: *Interflam 2019*. Egham, UK: Interscience Communications Ltd.; 2019:597-608.